

Evaluation of the Portal Imaging System Performance for an Elekta Precise Linac in Radiotherapy

Fateme Shahedi¹, Mahdi Momennezhad¹, Shahrokh Naseri^{1*}, Hamid Gholamhosseinian¹

1. Medical Physics Research Center, Mashhad University of Medical Sciences, Mashhad, Iran

ARTICLE INFO

Article type:
Original Article

Article history:
Received: Oct 18, 2017
Accepted: Feb 21, 2018

Keywords:
Quality Assurance
Radiotherapy
Imaging

ABSTRACT

Introduction: Electronic portal imaging devices (EPIDs) provide two- and three-dimensional planar and volumetric cone beam images to improve the accuracy of radiation treatment delivery. Periodic quality assurance (QA) of EPIDs is essential for dosimetric verification in radiotherapy. In this study, a QA program was implemented to evaluate the function of the EPID to be confident in applying corrections for the uncertainty of patient set-up.

Material and Methods: Firstly, the safety features were verified, and the uniformity of EPID response was evaluated using flat panel detector. Additionally, the contrast and spatial resolutions of the EPID were assessed using detail counting of the Los Vegas phantom images by visualization method and measuring the modulation transfer function using edge technique, respectively. Moreover, a combination of smoothing methods was used for optimal use of edge detection algorithm for the noisy portal images. Finally, the location of the central ray on the EPID surface at different gantry angles was determined to evaluate the mechanical stability of the supporting arm.

Results: The safety interlocks were found to be functional. The EPID response variation was less than 3% according to the results obtained from the detector. The contrast resolution met the recommended tolerance; however, the visualization method was widely observer-dependent. The value of f50 for spatial resolution was 0.401 ± 0.005 lp/mm for the photon energy of 6 MV. The supporting arm deviation was within ± 1 mm.

Conclusion: The periodic QA of image guidance system gave confidence to apply the corrections for set-up in clinic.

► Please cite this article as:

Shahedi F, Momennezhad M, Naseri Sh, Gholamhosseinian H. Effect of the Portal Imaging System Performance on the Precision of an Elekta Linear Accelerator in Radiotherapy. Iran J Med Phys 2018; 15: 295-303. 10.22038/ijmp.2018.27401.1287.

Introduction

Recently, developments in the construction of linear accelerators and using new imaging technologies have led to the creation of advanced radiation treatment techniques such as intensity modulated radiation therapy, volumetric modulated arc therapy, and image-guided radiation therapy (IGRT) [1, 2, 3]. The goal of all these techniques is to maximize radiation doses to tumor cells while minimizing damage to surrounding normal tissues. The verification of dose delivery and accurate patient positioning are essential to reach an appropriate treatment delivery [2, 3]. Electronic portal imaging devices (EPIDs), offers an effective method for this verifications [4]. In addition to traditional role of verifying patient set-up and planar dose mapping considered in the initial application of EPIDs [5-7], they are also used as a volumetric imaging modality in megavoltage cone beam computed tomography- (MV-CBCT) based IGRT. Image-guided MV-CBCT-based radiotherapy utilizes EPIDs mounted on linear accelerator to provide volumetric data for three-dimensional set-up verification to ensure the coincidence of treatment and planned isocenter [8, 9].

A regular quality assurance (QA) is needed to exploit the potentials of the EPID including the evaluation of the geometric uncertainties due to organ motion and set-up variations [10, 11]. In this regard, the American Association of Physicist in Medicine (AAPM) Task Group (TG)-142 has recommended a daily assessment of the collision interlocks and monthly check of geometric distortion. It is worth mentioning that the geometric distortion should not exceed 2 mm for non-stereotactic radiosurgery and stereotactic body radiotherapy (non-SRS/SBRT) [12]. Moreover, the AAPM TG-179 has recommended a monthly evaluation of image quality in the beginning, then a semiannual checking after the demonstration of parameter stability [13]. In this study, an amorphous silicon (a-Si) EPID with an active area of 41×41 cm² attached to an Elekta Precise Linear Accelerator (Elekta, Stockholm, Sweden), located at radiotherapy department of the Imam Reza Hospital affiliated to Mashhad University of Medical Sciences, Mashhad, Iran, was used.

The QA program consists of several tests, namely, system safety, uniformity assessment of EPID

response, image quality, and mechanical stability of the EPID supporting arm [8, 12-14]. Initially, the safety features were checked and the EPID calibration was performed to provide a uniform response for clinical imaging. Moreover, the uniformity of EPID response across the entire detector was measured by comparing the average pixel value of peripheral positions relative to the central position.

The low contrast resolution was evaluated using the contrast-detail counting of the Los Vegas phantom images by human observers [15]. Visualizing a certain hole in the Los Vegas phantom images demonstrates a low contrast resolution for a given imaging system [16]. The subjective process of detail counting of Los Vegas phantom images was insensitive to artifacts and observer-dependent. Furthermore, the modulation transfer function (MTF) of an EPID was determined by the edge-based technique to evaluate high spatial resolution [17].

Among all various methods proposed to calculate the presampled MTF for the imaging system such as edges, bar patterns, and slits [18, 19]. The edge method is more cost-effective and less sensitive to physical imperfections and misalignments of the test device [20]. The presampled MTF was deduced by fast Fourier transform of line spread function (LSF), which was obtained by the differentiation of the edge spread function (ESF).

Then, the spatial resolution was evaluated using the frequency at 50% of the presampled MTF. The implementation of a new combination of smoothing filters in ESF smoothing balanced data integrity and smoothing tradeoff for the noisy portal images that was not applied to the edge algorithm smoothing in previous studies. Finally, to evaluate the mechanical stability of the EPID supporting arm, the position of central ray on the detector was assessed using MATLAB software (MathWorks Inc., Natick, MA, USA, R2016A version) during a full gantry rotation.

The sagging shifts of the EPID supporting arm was mostly attributed to the heavy components of the head of the machine and mechanical structure of the supporting arm that has several sliding mechanical parts. Overall, this study was conducted to assess the quality assurance of the portal imaging system for verifying and correcting the patient set-up errors using planar or volumetric imaging technique prior to radiation delivery.

Materials and Methods

The Amorphous Silicon Based Electronic Portal Imaging Device

In this study, an Elekta Precise Linear Accelerator equipped with an a-Si based EPID (PerkinElmer Optoelectronics, Fremont, CA, USA) mounted on a mechanical arm was used. The mechanical arm holds the X-ray flat panel detector at a fixed source to detector distance (SDD) of 160 cm to obtain portal images. The flat panel detector has an active area of 41×41 cm² and

consisted of 1024×1024 pixels with a pixel size of 0.4 mm at the SDD of 160 cm.

The image detector encompassed field sizes up to 25.9×25.9 cm² at the isocenter plane. The a-Si detector could be divided into diverse layers including aluminum cover, air gap, 1 mm copper plate, graphite layer, scintillating phosphor screen, and active matrix array [21]. The EPID is connected to the iViewGT computer that provides synchronization between the detector and linear accelerator and also has software packages for signal processing [22]. The iViewGT system is an electronic system used for radiotherapy imaging, when attached to a linear accelerator; the system captures megavoltage portal images. The detector panel triggering, is controlled by the Detector Control Board (DCB), which is placed between the detector and computer, and is responsible for data transferring from the linear accelerator to the computer. This system uses the gun pulses from the linear accelerator to synchronize the detector reading; therefore, the pixels will be read when there is no radiation pulse, which improves the image quality [23]. The image data is sent directly to the frame grabber in the iViewGT system, where appropriate signal processing software packages automatically apply a set of corrections including gain and offset corrections to all images. Thereafter, a frame synchronization pulse is sent to the DCB. Accordingly, a combination of hardware and software is required to obtain portal images.

Safety Interlock

The flat panel detector is positioned by a robotic arm and rotates around the patient, creating a potential for collision between the EPID and patient support assembly. Collision sensors are installed between the detector and the outer cover. Exerting a low pressure on the outer cover activates the safety interlock. The collision safety interlock was checked by exerting a slight pressure on the four corners of the detector cover. The movement restriction of the gantry, couch, and flat panel imager with the activation of the safety interlocks was verified. Furthermore, the function of door interlock was checked by placing an object between the door sensors during irradiation that should terminate the beam.

Electronic Portal Imaging Device Calibration

The aim of EPID calibration is to remove the background noise and correct the detector pixel sensitivity to provide a uniform response for clinical images [24]. The detector calibration comprises of a dark field or offset image and a flood field image. Dark field image, which is used to correct background noise (offset correction), is provided by frame-averaging without any radiation delivery. The signal received from one readout of the entire matrix is called a frame.

In this study, at least 10 frames were allowed to be used for offset correction prior to the initiation of the radiation beam. Flood field image was obtained from the uniform irradiation of the entire detector at the photon energy of 6

MV to rectify variations in individual pixel sensitivities (gain correction). It is also the average of several frames similar to the dark field images. Each image is stored in the iViewGT local database. This software automatically applies these corrections to the images acquired by the EPID according to following equation:

$$\text{corrected image} = \left(\frac{EPID_{raw} - EPID_{DF}}{EPID_{FF}} \right) \overline{EPID_{FF}} \quad (1)$$

According to this equation, the pixel data in the EPID raw image $EPID_{raw}$ subtracted by the dark field image $EPID_{DF}$ and divided by the normalized gain correction image $EPID_{FF}$. $EPID_{FF}$ is the average value of flood field image used for image displaying.

Additionally, defected pixels that give inconsistent readings were corrected using a bad pixel map to improve the image quality. A pixel map for the defected pixels were identified through the acquisition of dark and flood fields. Once the defective pixels identified, the pixel values were set to an average of the neighboring pixel values [25].

Uniformity of Electronic Portal Imaging Device Response

In addition to the EPID calibration conducted by iViewGT software using dark and flood fields, EPID was irradiated for a field size of $20 \times 20 \text{ cm}^2$ with 10 monitor unit (MU) and a dose rate of 400 MU/min to ensure the uniformity of EPID response on different parts. The nominal SDD was 160 cm at the gantry angle of zero. As shown in Figure 1, the post-irradiation number of the region of interests (ROIs) with the size of 20×20 pixels was determined at the center and other parts of EPID.

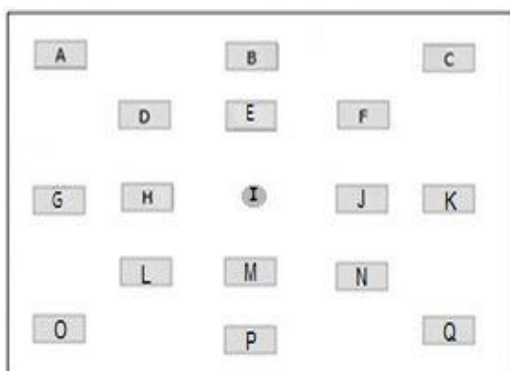


Figure 1. Specific locations of central and peripheral region of interests used to measure the uniformity response of electronic portal imaging devices within a $20 \times 20 \text{ cm}^2$ radiation field size. Each region of interest consists of 20×20 pixels.

The positional lengths at the detector level were $AB=BC=GI=IK=OP=PQ=11.2 \text{ cm}$ located at the outer beam, and $DE=DF=HI=IJ=LM=MN=6.4 \text{ cm}$ located at the inner beam of the irradiated field. The mean of the pixel values were determined for each of the ROIs and were compared with the mean pixel value of the central one. Error bars were calculated from the standard deviation of each ROI. The measurement was repeated three times under similar condition for a single photon

energy of 6 MV. The mean of the three images was determined and normalized to that of the central ROI. The EPID responses were analyzed with the help of MATLAB software R2016a (Mathworks Inc., Natick, Massachusetts, USA).

Image Quality

The parameters measured to describe the image quality of EPID included low contrast and spatial resolutions.

Low Contrast Resolution

The low contrast resolution was determined using the Los Vegas phantom, which was used in acceptance testing and QA (Figure 2) [16]. It consists of 27 holes with different thickness and depth embedded in an aluminum slab. To evaluate the contrast resolution of EPID, the Los Vegas phantom was set at the isocenter in a way that holes were facing down and irradiated at the field size of $12 \times 12 \text{ cm}^2$ and the dose rate of 200 MU/min at the gantry angle of zero. The phantom was irradiated with the photon energies of 6 MV, 10 MV, and 15 MV. The images were analyzed by visualization method, in which the number of holes implying contrast resolution was counted by three trained observers immediately after the acquisition. To evaluate the dependency of the process to observer, the measurement was repeated for the photon energy of 6 MV over 6 months.

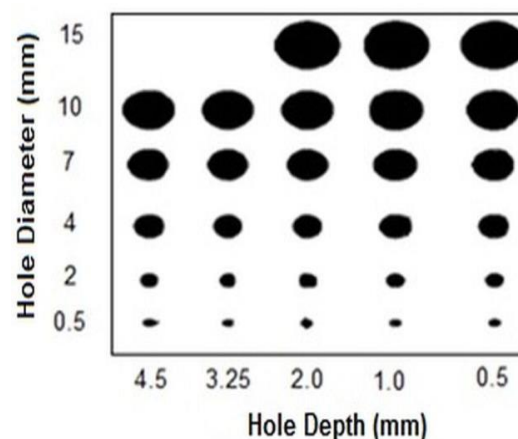


Figure 2. Schematic view of Los Vegas phantom.

High Contrast Resolution

The MTF was used to evaluate the resolution of the portal imaging system, which describes the resolution properties of the system as a function of spatial frequency [26]. The MTF was measured at the photon energy of 6 MV using the presampled MTF method described by Fujita et al. [27]. The edge block, which consists of aluminum with the dimensions of $20 \times 10 \times 1 \text{ cm}^3$ (thickness, length, and width, respectively) was placed on EPID surface at a shallow angle ($\alpha = 3^\circ$) with respect to the EPID pixel array.

The angulated positioning of the edge block allowed to increase sampling rate without aliasing effects [27-29]. At the first step, the edge orientation within each row was detected by applying Hough transform to the

image. The Hough transform is a technique utilized to identify the geometric features of images such as lines and curves. The main advantage of this technique is its ability to easily detect the background noise [30]. The next step is to determine a number of rows and columns in a given region for adequate representation of the ESF. In this study, the edge profiles of a group of 20 consecutive lines having one pixel distances from the first line to the last line were interleaved to construct oversampled ESF with data on sub-pixel level. The number of consecutive lines required across the edge was computed using following equation:

$$N = 1/(\tan \alpha) \quad (2)$$

It has not escaped our notice that “N” is the number of rows and columns and “ α ” is the tilt angle of the edge, which were indicated in the previous step [26, 27]. The sampling distance between adjacent pixels in the oversampled ESF is assumed to be equal and is given by dividing pixel pitch (Δx) to number of lines (N). Furthermore, noise reduction is important in the application of edge algorithm because it leads to both bias and variation errors in the estimation of the MTF. Several ESF smoothing methods such as average filtering and polynomial fit model were implemented in previous studies [31, 32]. In this study, careful consideration was made in the selection of the smoothing methods in order to keep a balance between smoothing and data integrity. Therefore, at the next step of the edge image analysis, ESF smoothing was performed by applying a combination of Gaussian and median filters to edge profiles to proceed the remaining processing with the minimal noise. In this study, a window size of 17 elements was used. To reveal data integrity in the smoothing process, the smoothed oversampled ESF was compared to the original oversampled ESF within the transition across the edge (Figure 3). This is due to the fact that the image quality of the imaging system corresponds to the distances of the transition region across the edge [33]. As demonstrated in Figure 3, the divergence of smoothed oversampled ESF from the original one on the edge transition region was within 0.002 mm. It was better than other smoothing methods implemented in previous studies such as polynomial fit algorithm and averaging filtering with the window width of 17, which revealed a divergence of 0.005 mm and 0.02 mm, respectively [34]. After being assured of nearly complete superposition of the results with the original data and therefore high data integrity during smoothing process, the oversampled smoothed ESF was differentiated to estimate the oversampled LSF. Ultimately, the presampled MTF was deduced by fast Fourier transfer of oversampled LSF and normalization of

its value to one at zero spatial frequency. The process, from finding edge orientation to oversampled LSF, is shown in Figure 4.

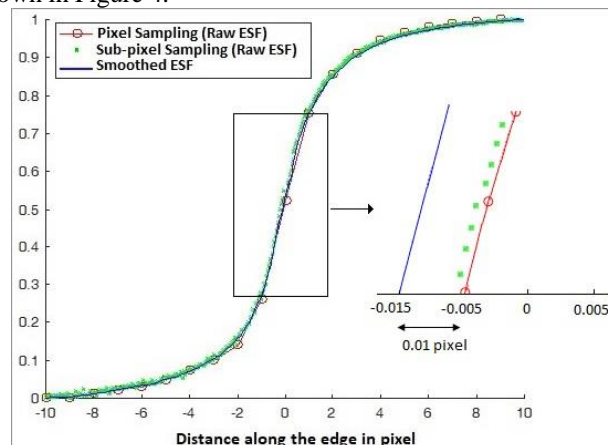


Figure 3. Divergence of the smoothed curve with the original data within the edge transition region.

Mechanical Support Arm Alignment

Gantry head is made of heavy components, which are affected by gravity during rotation; therefore, the accuracy of EPID positioning could be under the effect of gantry rotation, since the detector is mounted on a supporting arm with fasteners and gear belts [35]. With the growing application of EPIDs in pre- and post-treatment verification, and linear accelerator quality assurance processes in modern radiation therapy, it is essential to characterize and account for the mechanical system imperfections [36, 37].

Sagging shifts of the EPID supporting arm could degrade image quality and affect the accuracy of EPID-based mechanical and dosimetric QA [8, 35]. To evaluate the gravitational sag of supporting arm, several portal images for the field size of 10×10 cm² with 3 MU and dose rate of 200 MU/min were taken at different angles of gantry rotation (e.g., 0°, 45°, 90°, 135°, 180°, 225°, 270°, 315°, and 360°). The EPID was positioned at the SDD of 160 cm during full gantry rotations.

All images were taken in the 6 MV photon mode and then exported to the MATLAB software (R2016a) to find misalignment between the flat panel detector center and portal film center in X and Y (cross-plane and in-plane) directions. The measurement was conducted six times over a period of 6 month to assess the reproducibility of the results.

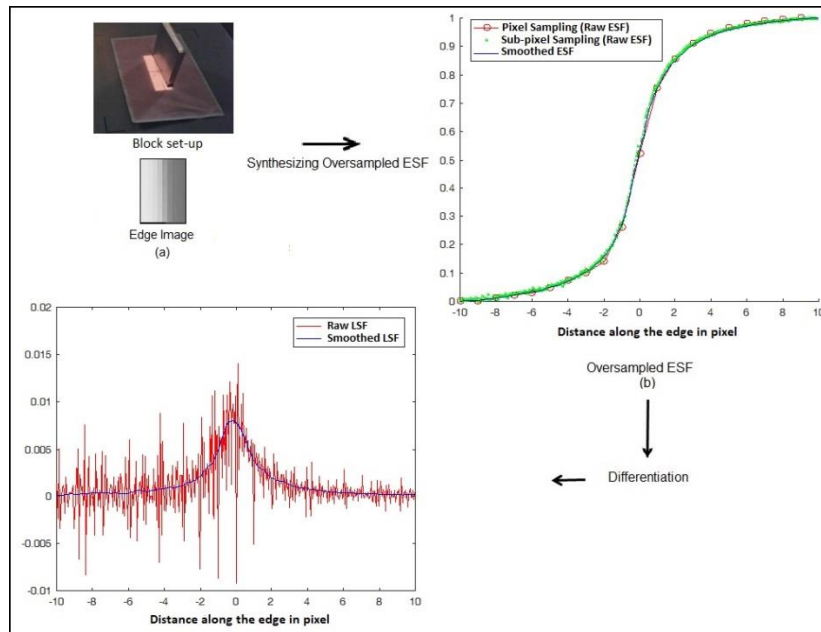


Figure 4. Processing steps from edge detection to obtaining oversampled edge spread function and line spread function

Results

Safety Interlock

The collision interlocks were found to be functional. The activation of the safety interlocks disabled the gantry, couch, and flat panel imager movements. The door interlock was functional when turn off the beam during imaging.

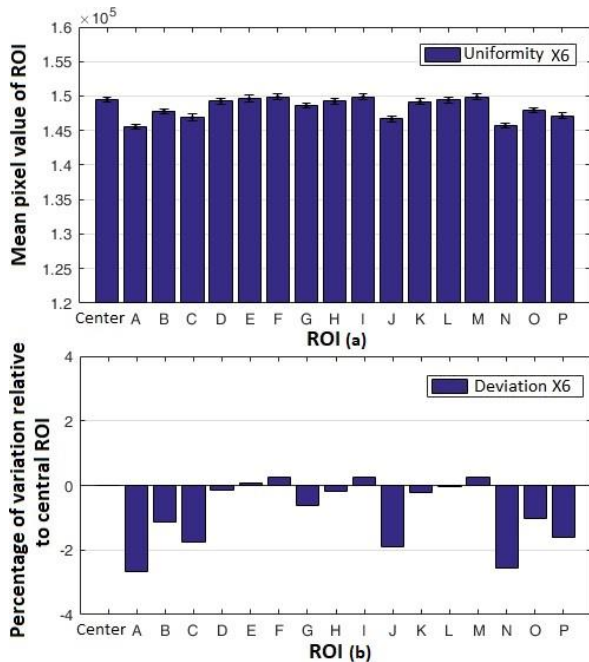


Figure 5. (a) Mean pixel value of central and peripheral region of interests within a $20 \times 20 \text{ cm}^2$ irradiated field, (b) the percentage of variation between mean pixel value of central and peripheral region of interests across the electronic portal imaging device.

Uniformity of Electronic Portal Imaging Device Response

The average pixel values of ROIs on different parts of field size ($20 \times 20 \text{ cm}^2$) and the percentage of variation between mean pixel value of central and peripheral ROIs are illustrated in Figure 5. With respect to the central ROIs, the pixel value of ROIs located close to the edge of irradiated field was slightly lower than others. The maximum variation between the mean pixel values of central and peripheral ROIs were less than 3% within the radiation field.

This is due to the offset and gain corrections applied automatically by the iViewGT software packages.

Low Contrast Resolution

The number of holes counted by three observers and inter-observer variability are plotted in Figure 6. Moreover, the variation in contrast-detail counting by human observers over 6 months for 6 MV photon energy is presented in Figure 7. Regarding the results, contrast resolution is improving over time. However, this is unexpected because of detector aging and is thought to be as a result of boosting the observer's confidence and offering training in identifying contrast details. Given the results, the number of counted holes was greater than the AAPM TG-58 recommended tolerance and met the manufacturer specifications [16, 38].

High Contrast Resolution

The modulation transfer function of the edge obtained by the Fourier transform of the oversampled LSF at 6 MV energy is shown in Figure 8. At zero frequency, the EPID had optimal performance in displaying large objects and the presampled MTF started at one (100%). The presampled MTF of the imaging system was reduced by 50% of its peak value at $0.401 \pm 0.005 \text{ lp/mm}$, which was the best metrics to

demonstrate image sharpness. There was an indirect relationship between the frequency increased and resolution.

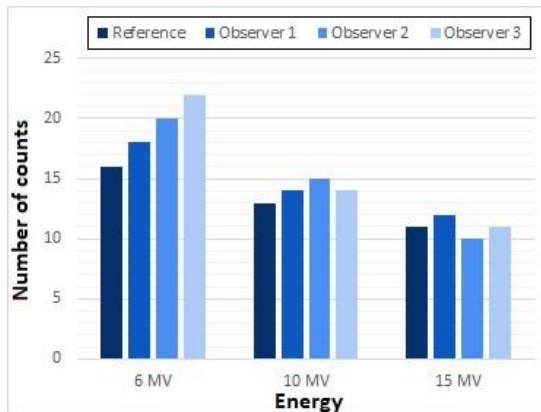


Figure 6. Number of holes detected by three trained observer

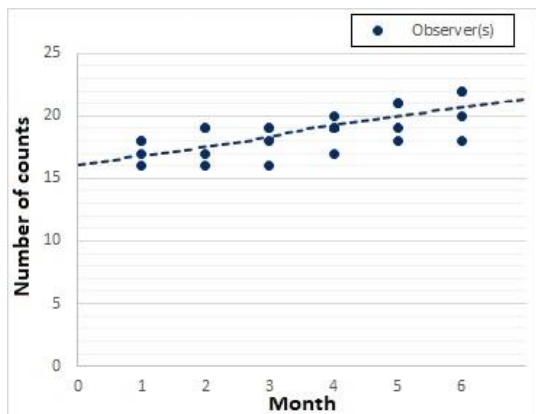


Figure 7. Las Vegas phantom test results for human observer over 6 months.

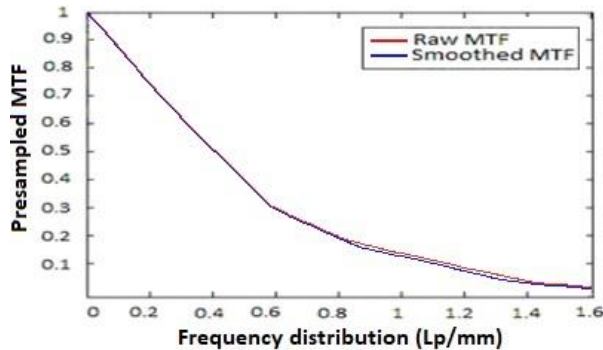


Figure 8. Presampled modulation transfer function obtained from the oversampled line spread function by Fourier transform.

The presampled MTF curve was decreased by 10% of its peak at 1.07 lp/mm, which was called the limiting spatial resolution. The large focal spot size employed for the most therapeutic linear accelerators contributed to a significant loss in spatial resolution and led to an incorporation of finite detector elements (pixels) to reduce the blurring effect. In addition, higher distance to the detector and lower SSDs will increase image

magnification and lead to geometric blurring enhancement due to X-ray focal spot. The optimal image magnification was found between 1.3 and 2.0 for nearly all portal imaging devices to achieve a high spatial resolution [39].

Mechanical Stability

The measured in- and cross-plane deviations between the flat panel detector center and portal film center at different gantry angles over 6 months are illustrated in Figure 9. According to the results, the EPID supporting arm deviation leading to the displacement of central ray on detector was in a repeatable manner over time. The maximum measured deviation was 0.25 mm in the cross-plane direction, while larger deviations were observed in the in-plane direction. However, the measured values were all within 2 mm, which is the accepted criterion for non-stereotactic linear accelerators, as noted in AAPM TG-142 [12].

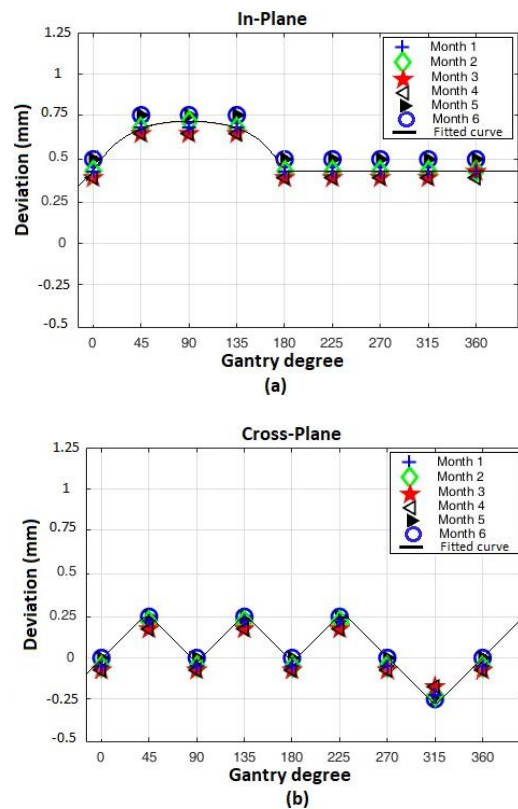


Figure 9. The results of in-plane (a), and cross-plane (b) deviations between detector center and portal image center at different gantry angles over 6 months.

Discussion

In this study, we performed a QA program including system safety, uniformity of EPID response, image quality, and mechanical stability of the supporting arm to evaluate the performance of the portal imaging system on Elekta Precise Linear Accelerator in order to be used for treatment verification. The daily check of the function of the system safety interlocks is required. Furthermore, the manufacturer sometimes provides

override buttons to bypass the interlocks that should be checked periodically for safe clinical use [40].

Pixel-response uniformity across the flat panel detector, is considered as one of the important factors affecting both the imaging and dosimetric performance of the EPID. Regarding the results of the present study, the EPID uniformity was about 97% across the entire detector with a maximum deviation of 2.8% from the central ROI. This result was in agreement with that reported by Kavuma Awusi [41].

Periodic gain calibration and defective pixel map correction of the flat panel detector is required to provide a uniform response for optimal image quality performance. Low and high contrast resolutions were determined to evaluate megavoltage image quality. The main limitation of visualization method in detail counting was the dependency of the process to the display system performance, observer training, and viewing conditions. However, according to the literature, the automatic methods that detect the structures based on the difference between gray scale of each hole with its background are robust and fully objective [42].

The results of the current study for low contrast resolution were superior to those reported by TG-58 [16]. The spatial resolution f50 was 0.401 ± 0.005 lp/mm, which was less than that reported by Clement et al. (0.461 lp/mm) for the Elekta iViewGT. In the mentioned study, the spatial resolution was measured using bar pattern phantom at 6 MV photon energy [43]. One of the important points that should be considered in the edge response method is that the calculated LSF and the resultant MTF may have some degree of uncertainty that comes from the experimental data noise. It is due to the high sensitivity of the first derivative to fluctuations in the experimental data [44].

The implementation of a consecutive filtering approach in the edge algorithm was determined to provide optimal data smoothing for the noisy portal images, while maintaining data integrity. The quality of megavoltage images is not as good as the kilovoltage X-ray beam images. Nonetheless, megavoltage images provide sufficient contrast to assess bony structures and soft tissues for target delineation and patient position verification. There are many factors contributing to the poor quality of megavoltage images including focal spot size of the X-ray tubes, the performance of image receptor, and Compton scattering as a predominant interaction in the megavoltage energy range.

A high quality image guidance requires higher MU protocol which led to additional exposure of the patient and should be incorporated into treatment planning process. Generally, there is a trade-off between low-contrast detectability and high contrast resolution for a given dose in IGRT. Due to the higher importance of low-contrast detectability in IGRT, high contrast resolution is somewhat compromised [45].

Because the mechanical alignment of the flat panel detector with treatment beam is essential for the verification of patient treatment position, check of the

mechanical stability is considered as the most important test. Heavy components of the head of machine affecting by the gravity during gantry rotation, the mechanical structure of the supporting arm including joints, gear belts, and the age of EPID are considered as the main causes of instability in the supporting arm [46].

The simple and time-saving method employed for evaluating the mechanical stability of the supporting arm does not need further costs for QA equipment and has no limitations associated with phantom measurement techniques such as high accuracy phantom aligning at the isocenter. The results of the supporting arm sag measurement at different gantry angles showed that the maximum deviation in the in- and cross-plane directions were 0.75 mm and 0.25 mm, respectively. The capability of moving more freely in the in-plane directions due to the presence of a joint in the arm structure results in larger deviation in comparison to the cross-plan direction. Our results were in line with another study conducted on Elekta Linear Accelerator [46].

Conclusion

The planar and volumetric X-ray image guidance procedures are routine in the clinical radiotherapy; therefore, the periodic QA is essential to verify the integrity of these system. In this study, we implemented the QA program to evaluate the functionality of the iViewGT portal imaging device. Given the results, the performance of the Elekta Precise Linear Accelerator was accurate for treatment verification and met the expectations consistent with patient care requirements.

Acknowledgment

The authors would like to thank Mr. Amir Zamanpour for his technical support.

References

1. O'Daniel JC, Garden AS, Schwartz DL, Wang H, Ang KK, Ahamad A, et al. Parotid gland dose in intensity-modulated radiotherapy for head and neck cancer: is what you plan what you get?. *International Journal of Radiation Oncology* Biology* Physics*. 2007;69(4):1290-6.
2. Bedford JL. Treatment planning for volumetric modulated arc therapy. *Medical physics*. 2009;36(11):5128-38.
3. Fredh A, Korreman S, af Rosenschöld PM. Automated analysis of images acquired with electronic portal imaging device during delivery of quality assurance plans for inversely optimized arc therapy. *Radiotherapy and Oncology*. 2010;94(2):195-8.
4. Kirby M, Glendinning A. Developments in electronic portal imaging systems. *The British journal of radiology*. 2014.
5. Van Herk M, Meertens H. A matrix ionisation chamber imaging device for on-line patient setup verification during radiotherapy. *Radiotherapy and Oncology*. 1988;11(4):369-78.

6. Heijmen B, Pasma K, Kroonwijk M, Althof V, De Boer J, Visser A, et al. Portal dose measurement in radiotherapy using an electronic portal imaging device (EPID). *Physics in medicine and biology*. 1995;40(11):1943.
7. Das IJ, Cao M, Cheng C-W, Mistic V, Scheuring K, Schule E, et al. A quality assurance phantom for electronic portal imaging devices. *Journal of Applied Clinical Medical Physics*. 2011;12(2).
8. Midgley S, Millar R, Dudson J. A feasibility study for megavoltage cone beam CT using a commercial EPID. *Physics in medicine and biology*. 1998;43(1):155.
9. Bissonnette J-P, editor *Quality assurance of image-guidance technologies. Seminars in radiation oncology*; 2007: Elsevier.
10. Tournel K, De Ridder M, Engels B, Bijdekerke P, Fierens Y, Duchateau M, et al. Assessment of intrafractional movement and internal motion in radiotherapy of rectal cancer using megavoltage computed tomography. *International Journal of Radiation Oncology* Biology* Physics*. 2008;71(3):934-9.
11. Gopal A, Samant SS. Use of a line-pair resolution phantom for comprehensive quality assurance of electronic portal imaging devices based on fundamental imaging metrics. *Medical physics*. 2009;36(6):2006-15.
12. Klein EE, Hanley J, Bayouth J, Yin FF, Simon W, Dresser S, et al. Task Group 142 report: quality assurance of medical accelerators. *Medical physics*. 2009;36(9):4197-212.
13. Bissonnette JP, Balter PA, Dong L, Langen KM, Lovelock DM, Miften M, et al. Quality assurance for image-guided radiation therapy utilizing CT-based technologies: A report of the AAPM TG-179. *Medical physics*. 2012;39(4):1946-63.
14. Kanakavelu N, Samuel EJ. Assessment and evaluation of MV image guidance system performance in radiotherapy. *Reports of Practical Oncology & Radiotherapy*. 2015 May 1;20(3):188-97.
15. Low DA, Klein EE, Maag DK, Umfleet WE, Purdy JA. Commissioning and periodic quality assurance of a clinical electronic portal imaging device. *International Journal of Radiation Oncology· Biology· Physics*. 1996 Jan 1;34(1):117-23.
16. Herman MG, Balter JM, Jaffray DA, McGee KP, Munro P, Shalev S, et al. Clinical use of electronic portal imaging: report of AAPM Radiation Therapy Committee Task Group 58. *Medical Physics*. 2001;28(5):712-37.
17. Smith PL. New technique for estimating the MTF of an imaging system from its edge response. *Applied Optics*. 1972 Jun 1;11(6):1424-5.
18. Rout BK, Shekar MC, Kumar A, Ramesh KK. Quality control test for electronic portal imaging device using QC-3 phantom with PIPSPRO. *International Journal of Cancer Therapy and Oncology*. 2014 Sep 29;2(4).
19. Cunningham IA, Reid BK. Signal and noise in modulation transfer function determinations using the slit, wire, and edge techniques. *Medical physics*. 1992 Jul 1;19(4):1037-44.
20. E. Samei, M. Flynn and D. Reimann, A method for measuring the presampled MTF of digital radiographic systems using an edge test device. *Medical Physics*. 1998;25: 102-13.
21. Gustafsson H, Vial P, Kuncic Z, Baldock C, Greer PB. EPID dosimetry: Effect of different layers of materials on absorbed dose response. *Medical physics*. 2009 Dec 1;36(12):5665-74.
22. Winkler P, Hefner A, Georg D. Dose-response characteristics of an amorphous silicon EPID. *Medical physics*. 2005 Oct 1;32(10):3095-105.
23. Van der Sypt, Jan, Carlos De Wagter, and Luc Van Hoorebeke. EPID based quality assurance of Total Body Irradiation. Master [dissertation]. Belgium: Ghent university. 2016.
24. Sukumar P, Padmanaban S, Jeevanandam P, Kumar SS, Nagarajan V. A study on dosimetric properties of electronic portal imaging device and its use as a quality assurance tool in Volumetric Modulated Arc Therapy. *Reports of Practical Oncology & Radiotherapy*. 2011;16(6):248-55.
25. Balter JM, Antonuk LE. Quality Assurance for kV and MV In-room Imaging and Localization for Off-and Online Setup Error Correction. *International journal of radiation oncology, biology, physics*. 2008;71(1 Suppl): 48-52.
26. Buhr E, Günther-Kohfahl S, Neitzel U. Accuracy of a simple method for deriving the presampled modulation transfer function of a digital radiographic system from an edge image. *Medical physics*. 2003;30(9):2323-31.
27. Fujita H, Tsai D-Y, Itoh T, Doi K, Morishita J, Ueda K, et al. A simple method for determining the modulation transfer function in digital radiography. *IEEE Transactions on medical imaging*. 1992;11(1):34.
28. Greer PB, Van Doorn T. Evaluation of an algorithm for the assessment of the MTF using an edge method. *Medical Physics*. 2000;27(9):2048-59.
29. Marshall N. Early experience in the use of quantitative image quality measurements for the quality assurance of full field digital mammography x-ray systems. *Physics in medicine and biology*. 2007;52(18):5545.
30. Hassanein AS, Mohammad S, Sameer M, Ragab ME. A survey on Hough transform, theory, techniques and applications. *arXiv preprint arXiv:1502.02160*. 2015 Feb 7.
31. Carton AK, Vandenbroucke D, Struye L, Maidment AD, Kao YH, Albert M, et al. Validation of MTF measurement for digital mammography quality control. *Medical Physics*. 2005 Jun 1;32(6Part1):1684-95.
32. Saunders RS, Samei E. A method for modifying the image quality parameters of digital radiographic images. *Medical physics*. 2003 Nov 1;30(11):3006-17.
33. B. Hasegawa, *The Physics of Medical X-Ray Imaging*, Madison, Wisconsin: Medical Physics Publishing Company. 1990.
34. Donovan M, Zhang D, Liu H. Step by step analysis toward optimal MTF algorithm using an edge test device. *Journal of X-ray science and technology*. 2009 Jan 1;17(1):1-5.
35. Rowshanfarzad P, McGarry CK, Barnes MP, Sabet M, Ebert MA. An EPID-based method for comprehensive verification of gantry, EPID and the MLC carriage positional accuracy in Varian linacs

- during arc treatments. *Radiation Oncology*. 2014;9(1):249.
36. Bailey DW, Kumaraswamy L, Bakhtiari M, Malhotra HK, Podgorsak MB. EPID dosimetry for pretreatment quality assurance with two commercial systems. *Journal of applied clinical medical physics*. 2012 Jul 1;13(4):82-99.
 37. Sun B, Goddu SM, Yaddanapudi S, Noel C, Li H, Cai B, Kavanaugh J, Mutic S. Daily QA of linear accelerators using only EPID and OBI. *Medical physics*. 2015 Oct 1;42(10):5584-94.
 38. Elekta Customer Acceptance tests for iViewGT. Document number: 45133701945 04. Elekta company; 2008.
 39. Bissonnette JP, Jaffray DA, Fenster A, Munro P. Optimal radiographic magnification for portal imaging. *Medical physics*. 1994 Sep 1; 21(9):1435-45.
 40. Levitt SH, Purdy JA, Perez CA, Vijayakumar S. *Technical basis of radiation therapy*. 4th ed. Minnesota: Springer. 2012; 104.
 41. Kavuma A. Transit dosimetry based on water equivalent path length measured with an amorphous silicon electronic portal imaging device: University of Glasgow; 2011.
 42. Jomehzadeh A, Shokrani P, Mohammadi M, Amouheidari A. A quality assurance program for an amorphous silicon electronic portal imaging device using in-house developed phantoms: A method development for dosimetry purposes. *Int J Radiat Res*. 2014 Jul 1; 12: 257-64.
 43. Clements R, Luchka K, Pouliot J, Sage J, Shalev S. Initial comparison of three Am-Si EPIDs using the QC-3V Phantom. The 7th international workshop on electronic Portal Imaging-EPI2K2; 2002.
 44. Doi K. Basic imaging properties of radiographic systems and their measurement. In: Orton C. *Progress in medical radiation physics*. 2th ed. Chicago (IL): Springer US. 1985: 181-248.
 45. JJ. Sonke. In-room imaging techniques. In: KK. Brock. *Image Processing in Radiation Therapy* [e-book]. Michigan: CRC Press; 2013 [cited 2015 February 3]. Available from : Wiley Online Library.
 46. Rowshanfarzad P, Riis H, Zimmermann S, Ebert M. A comprehensive study of the mechanical performance of gantry, EPID and the MLC assembly in Elekta linacs during gantry rotation. *The British journal of radiology*. 2015;88(1051):20140581.